Sixth International Symposium on Marine Propulsors
smp'19, Rome, Italy, May 2019

A New Design Method for Ship Propellers with Prescribed Circulation Distributions Based on the Vortex Lattice Lifting-Surface Model

Chen-Jun Yang, Qi Wang, Xiao-Qian Dong, Wei Li, Francis Noblesse

State Key Laboratory of Ocean Engineering, Shanghai Jiao Tong University, Shanghai, China.

ABSTRACT

A new design method has been developed for ship propellers with prescribed circulation distributions based on the vortex lattice lifting-surface model (VLM). For a given set of camber surface geometry and pitch profile of the blade, the circulation distribution in a uniform or a radially non-uniform inflow is computed by means of the VLM, and used to update the camber surface geometry by the Newton-Raphson iterative scheme according to the differences between the computed and the prescribed circulation distributions. Numerical examples are given to confirm that the converged camber surface geometry and pitch profile are practically independent of the initial values, and the method converges well with the number of vortex lattices along the span and the chord. The present method has been applied to design a highly skewed propeller in open water. The hydrodynamic performance and blade-surface pressure distributions of the designed propeller are numerically verified by means of RANS simulation.

Keywords

Propeller, design, lifting surface, vortex lattice.

1 INTRODUCTION

Propeller design is a fundamental problem. Nowadays, ship propellers are mostly designed by means of numerical methods and model experiments, in order to compromise better among competing performances, such as propulsive efficiency and cavitation. Hence it is always desirable to develop accurate and robust methods for propeller design. However, except for the several classical methods known to all the community, the research of propeller design methods seems to be insufficient.

As is well known, most methods for propeller design are based on one of the three potential-flow models for the finite-span wing. Lerbs (1952) proposed a lifting-line design method for moderately loaded propellers, where the circulation distribution may be optimal or prescribed, and the inflow may be uniform or radially non-uniform. This method was improved by introducing the lifting surface corrections, owing to the contributions from Lerbs (1955), Kerwin *et al*. (1963), Cheng (1965), and Morgan *et al*. (1968). Pien (1961) proposed a design method based on the lifting surface model, where the vortex distribution was treated as a continuous function. A major advance in lifting surface theory was made by Kerwin and Lee (1978), where the vortex distributions were represented by discrete vortex lattices, offering great flexibility in the treatment of highly skewed propeller geometry. The vortex lattice method for propeller design was proposed by Greeley and Kerwin (1982), where the blade geometry was determined iteratively by diminishing the normal velocity residuals. Tan *et al*. (2005) represented the camber surface with B-splines, and solved the design problem by the method of least squares. Su and Ikehata (1999) proposed a surface panel method to design the propeller according to prescribed pressure distributions. This design method is theoretically more accurate than the lifting-line and lifting-surface methods. However, it is not widely used up to date, probably due to the difficulties associated with the prescription of pressure distributions. In recent years, there is a steady increase in the attempt to design marine propellers by means of optimization methods. This is a trend, however, a substantial growth in computer power seems to be crucial for the optimization methods to be practical, even if the lifting-surface or surface-panel models are employed to evaluate propeller performances.

At present, it seems to be a usual practice to perform a preliminary design by the lifting-line model, and a detailed design by the lifting-surface model. The design results can be further refined by performing surface-panel or viscous-flow CFD simulation. Obviously, the accuracy of lifting-surface design becomes very important in such a design flow. In this paper, the lifting-surface design of the propeller subject to a prescribed circulation distribution is considered, aiming at better accuracy and smoothness in the geometry designed.

2 DESIGN METHOD

2.1 General description

In this study, design of the propeller at a given advance ratio (J) is considered. The inflow can be uniform or axisymmetrical. The radial distributions of blade chord length, skew angle, and rake are known. The radial and chordwise thickness distributions are also given. These geometrical data are typically determined in the lifting-line design. Hence the present design task is reduced to

the determination of blade camber surface geometry and pitch distribution. In addition, the circulation distribution over the camber surface is prescribed in the present design method. The problem of optimizing the circulation distribution along the radius can be treated separately.

The present design method is based on the vortex lattice lifting-surface model (VLM). It is simply composed of two steps,

1) For a given set of camber surface geometry and pitch distribution, perturb the camber or the pitch once at a location and solve a steady performance problem to evaluate variations in circulation due to the perturbation. The Jacobian matrix is built by making perturbations over the camber surface.

2) Update the camber and pitch distributions according to the differences between the circulation distribution of the present blade geometry and that prescribed, by means of the Newton-Raphson method.

The present method is different from the classical VLM design method by Greeley and Kerwin (1982). The latter also begins with an assumed blade geometry. Instead of solving a steady flow problem, the spanwise vortices with prescribed strengths are arranged on the assumed camber surface, and the velocities induced by the singularity systems are calculated. The assumed camber surface geometry and pitch distribution are updated according to the residual velocity normal to the camber surface, and the final geometry is obtained when the normal velocity vanishes.

2.2 Discretization

2.2.1 Camber surface

As illustrated in Figure 1, the propeller rotates about the *x*-axis at a constant angular speed Ω. The camber surface is first discretized from the root to the tip by M+1 concentric cylinders at the radii

$$r_m^v = r_H + (R - r_H)\frac{4m-3}{4M+2} \quad (m = 1, 2, ..., M+1) \qquad (1)$$

where r_H and R denote the root radius and the tip radius, respectively.

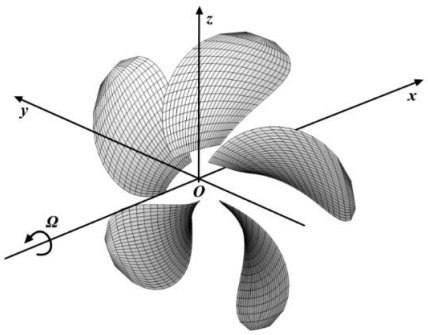

Figure 1. Vortex lattice model for camber surfaces.

Then, the strip of camber surface between r_m^v and r_{m+1}^v is further discretized along the chord into N quadrilateral lattices by

$$s_n = (n-1)/N \quad (n = 1, 2, ..., N+1) \qquad (2)$$

where s is the non-dimensional chordwise coordinate, s=0 at the leading edge, and s=1 at the trailing edge.

The ends of the $(m,n)^{\text{th}}$ spanwise vortex are located at (r_m^v, s_n^v) and (r_{m+1}^v, s_n^v), where $m = 1, 2, ..., M$, and

$$s_n^v = s_n + \tfrac{1}{4}(s_{n+1} - s_n) \quad (n = 1, 2, ..., N) \qquad (3)$$

The $(i,j)^{\text{th}}$ control point is located at (r_i^c, s_j^c), where

$$\left.\begin{aligned} r_i^c &= (r_i^v + r_{i+1}^v)/2 \qquad (i = 1, 2, ..., M) \\ s_j^c &= s_j + \tfrac{3}{4}(s_{j+1} - s_j) \quad (j = 1, 2, ..., N) \end{aligned}\right\} \qquad (4)$$

According to Kerwin and Lee (1978), this arrangement of the spanwise vortices and control points satisfies the Kutta condition at the trailing edge implicitly.

2.2.2 Trailing vortex wake

The trailing vortex wake is modeled with discrete vortex lines emanating from the ends of the spanwise vortex elements. Theoretically the trailing vortex lines should be parallel to the local flow since they are force-free. But this condition is difficult to fulfill since the trailing vortex strength and geometry are both unknown. Hence it is a usual practice to prescribe the trailing vortex geometry via the so-called wake model.

In this paper, the wake model proposed by Yang *et al.* (1990) is adopted. The propeller slipstream is divided into the near wake and the far wake. The near wake begins from the trailing edge and extends 1*D* downstream; then the far wake begins, and it ends at 8*D* downstream of the trailing edge. Here *D* denotes the propeller diameter. Both the trailing vortex pitch angle and radius vary linearly with the angular coordinate in the near wake, but become constant in the far wake. At the entrance of the near wake, the trailing vortex pitch angle and radius are, respectively

$$\left.\begin{aligned} \beta_{ws}(r_m^v) &= 0.5\left[\phi(r_m^v) + \beta_I(r_m^v)\right] \\ r_{ws}(r_m^v) &= r_m^v \end{aligned}\right\} \qquad (5)$$

where ϕ and β_I denote the geometric pitch angle and the advance angle, respectively. At the end of the near wake and in the far wake, the trailing vortex pitch angle is estimated as

$$\beta_{we}(r_m^v) = \phi(r_m^v) \qquad (6)$$

The radii of the trailing vortices shedding from the root and the tip are, respectively,

$$\left.\begin{aligned} r_{we}(r_1^v) &= 0.05R \\ r_{we}(r_{M+1}^v) &= (0.78 \sim 0.95)R \end{aligned}\right\} \qquad (7)$$

The trailing vortices shedding from the other sections $(r_2^v, r_3^v, ..., r_M^v)$ are assumed to be equally spaced in radial direction. Figure 2 shows an example of the trailing vortex geometry.

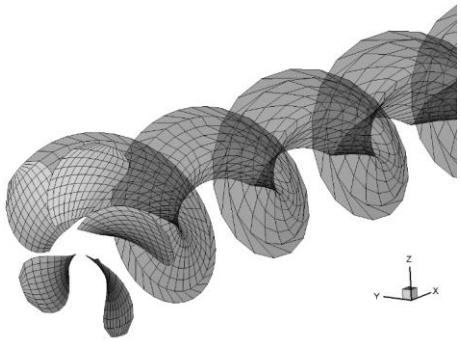

Figure 2. Trailing vortex geometry.

2.3 Design procedure

2.3.1 Prescribed strength of spanwise vortex

The radial distribution of circulation, $\Gamma(r)$, is an input in the present method. To prescribe the spanwise vortex strengths, the NACA a=0.8 loading distribution is used along the chord. The surface density of spanwise vortex is expressed as

$$\gamma(r,s)=\begin{cases}\bar{\gamma}(r) & (s\le 0.8)\\ 5\bar{\gamma}(r)\cdot(1-s) & (0.8<s\le 1.0)\end{cases} \tag{8}$$

where $\bar{\gamma}(r)=\Gamma(r)/[0.9C(r)]$, $\Gamma(r)$ and $C(r)$ are, respectively, the total circulation and chord length of the blade section at radius r. The prescribed (target) strength of the $(m,n)^{\text{th}}$ spanwise vortex is

$$\Gamma^{o}_{mn}=\frac{C(r^{c}_{m})}{N}\int_{s_n}^{s_{n+1}}\gamma(r^{c}_{m},s)ds \tag{9}$$

2.3.2 Jacobian matrix

The camber f_{ij} at $M\cdot(N-1)$ locations (circles in Figure 3) and the pitch angle ϕ_i at M sections (dashed arcs in Figure 3) are chosen as design variables, where $f_{ij}=f(r^{c}_{i},s^{v}_{j})$, $\phi_i=\phi(r^{c}_{i})$. The total number of design variables is $L=M\cdot N$.

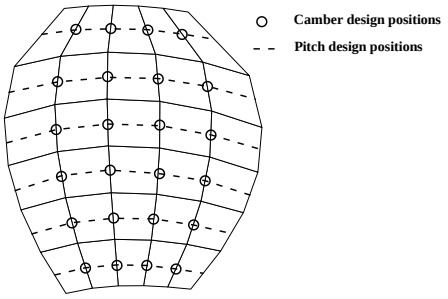

Figure 3. Arrangement of design variables.

To simplify the expression, let

$$\chi_\beta=\begin{cases} f_{ij} & \begin{pmatrix}\beta=j+(i-1)\cdot N,\\ i=1,2,\text{L}\ ,M,\\ j=1,2,\text{L}\ ,N-1.\end{pmatrix}\\ \phi_i & \begin{pmatrix}\beta=i\cdot N,\\ i=1,2,\text{L}\ ,M.\end{pmatrix}\end{cases} \tag{10}$$

For a known blade geometry, the $(m,n)^{\text{th}}$ spanwise vortex strength is denoted by Γ_α , where $\alpha=n+(m-1)\cdot N$, $m=1,2,...,M$, $n=1,2,...,N$, and $\alpha=1,2,...,L$. The spanwise vortex strengths are obtained by predicting the steady performance using an in-house VLM code, which will be briefly described in Section 2.3.4. Similarly, the target strength Γ^{o}_{mn} defined in (9) is now written as Γ^{o}_{α}. Then the design objective is expressed as

$$\Delta\Gamma_\alpha=\Gamma_\alpha-\Gamma^{o}_{\alpha}=0 \tag{11}$$

The design objective is an implicit function of the design variables, *i.e.*

$$\Delta\Gamma_\alpha=F_\alpha(\chi_1,\chi_2,\cdots,\chi_L)$$

The variation in the α^{th} spanwise vortex strength due to perturbation to the β^{th} design variable is evaluated as

$$\frac{\partial(\Delta\Gamma_\alpha)}{\partial\chi_\beta}\approx\frac{\Delta F_{\alpha\beta}}{\Delta\chi_\beta} \tag{12}$$

where

$$\Delta F_{\alpha\beta}=F_\alpha(\chi_1,\chi_2,\cdots,\chi_\beta+\Delta\chi_\beta,\cdots,\chi_L)-F_\alpha(\chi_1,\chi_2,\cdots,\chi_\beta,\cdots,\chi_L)$$

Let $\alpha,\beta=1,2,...,L$, (12) constitutes $\boldsymbol{J}$, a Jacobian matrix of order L. The amount of perturbation to the design variable is $\Delta\chi_\beta=0.01\chi_\beta$ $(\beta=1,2,...,L)$. It is most time consuming to establish the Jacobian matrix, since one needs to solve a steady performance problem for the perturbation of each design variable. Fortunately, it turns out that the Jacobian matrix established initially can be used throughout the iteration process without affecting the design results.

2.3.3 Update of design variables

According to the Newton-Raphson method, the design variables are updated iteratively by

$$\boldsymbol{\chi}^{(k+1)}=\boldsymbol{\chi}^{(k)}-\left(\boldsymbol{J}^{(k)}\right)^{-1}\Delta\boldsymbol{\Gamma}^{(k)} \tag{13}$$

where $\boldsymbol{\chi}=(\chi_1,\chi_2,\text{L}\ ,\chi_L)^T$, $\Delta\boldsymbol{\Gamma}=(\Delta\Gamma_1,\Delta\Gamma_2,\cdots,\Delta\Gamma_L)^T$, and the superscripts in brackets denote the number of iterations.

2.3.4 Solution of steady performance problem

When the propeller geometry is known, the blades are replaced with a set of horseshoe vortices located on the camber surfaces and in the slipstream, according to the discretization schemes described in Section 2.2. The thickness of blade is simulated with line source/sink elements that are located on the camber surface, too.

By fulfilling the non-penetration condition, a set of linear algebraic equations for the unknown spanwise vortex strengths, Γ_{mn}, are established as follows,

$$\sum_{k=1}^{Z}\sum_{m=1}^{M}\left\{\sum_{n=1}^{N}\left[K^{s}_{ijmnk}+\sum_{p=n}^{N}\left(K^{c}_{ij(m+1)pk}-K^{c}_{ijmpk}\right)+\sum_{p=1}^{N_w}\left(K^{w}_{ij(m+1)pk}-K^{w}_{ijmpk}\right)\right]\right\}\Gamma_{mn}+\left(\boldsymbol{V}_I+\boldsymbol{V}_Q\right)_{ij}\cdot\boldsymbol{n}_{ij}=0 \quad (14)$$

where Z is the number of blades, N_w is the number of straight-line elements used to discretize a vortex line; the K's denote the normal component of velocity induced by a line vortex element of unit strength; the superscripts s, c, and w denote the spanwise, chordwise, and trailing vortex elements, respectively; the subscripts i and j denote the $(i,j)^{\text{th}}$ control point where the induced velocity is calculated, while the subscripts m, n, and k denote the $(m,n)^{\text{th}}$ vortex element of the k^{th} blade by which the velocity is induced. The subscripts i, m=1, 2, ..., M; j, n=1, 2, ..., N. The relative inflow velocity is denoted by $\boldsymbol{V}_I$, the velocity induced by all the source/sink elements by $\boldsymbol{V}_Q$., and the unit normal vector to the camber surface by $\boldsymbol{n}$.

After the spanwise vortex strengths are obtained by solving the linear equations, the steady thrust and torque acting on the propeller are calculated. For details see Yang *et al*. (1990).

3 RESULTS AND DISCUSSION

The DTNSRDC-4382 propeller is used to investigate the convergence properties and accuracy of the present design method. The propeller, renamed as P4382 hereinafter, is five-bladed and has a max. skew angle of 36 degrees. The geometric data of P4382 is available in Kerwin and Lee (1978). The design point of P4382 is J=0.889.

3.1 Grid dependency

The radial distribution of circulation, $\Gamma(r)$, is predicted first by solving the steady performance problem of P4382 at the design point, and adopted as the prescribed one for the design. Then the P4382 is re-designed. The initial pitch angle is equal to the angle of advance, while the initial camber is set to zero. Ideally, the re-design should reproduce the pitch and camber distributions of P4382.

Nine combinations of spanwise division number M and chordwise division number N are used to investigate the grid dependency, where M=9, 14, 19 and N=15, 20, 25, respectively. Figure 4 shows that the re-designed pitch and camber distributions converge very fast with the size of vortex lattices, and agree well with those of P4382. Figure 5 shows that the re-designed camber surface (with M=14 and N=20) is very smooth and quite close to that of P4382. The slight differences are attributable to the fact that the NACA a=0.8 loading distribution is strictly enforced in the re-design, but possibly not so for P4382. Based on the investigation, M=14, N=20 is recommended and will be used in the following numerical examples.

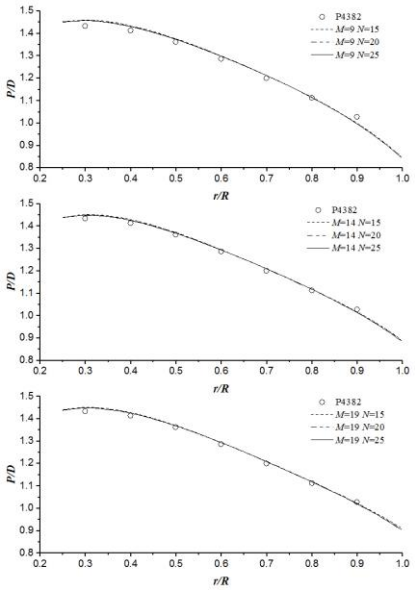

(a) Pitch distribution

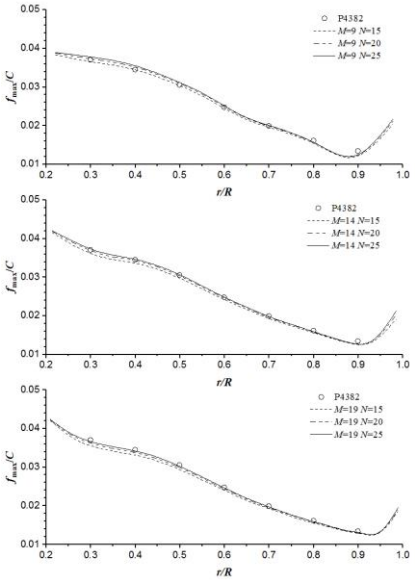

(b) Max. camber distribution

Figure 4. Comparison of re-designed and original pitch and camber distributions.

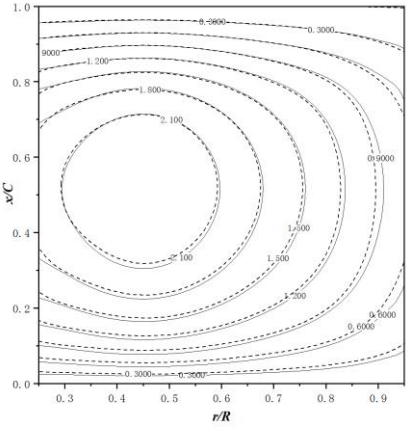

Figure 5. Comparison of re-designed (dashed) and original (solid) camber surface geometries.

3.2 Initial-value dependency and convergence speed

Since the pitch and camber distributions are iteratively determined, it is beyond doubt that the design results must be independent of the initial value. In practice, the initial pitch and camber can be quite rationally guessed, such as the following,

Case A: $P/D=J$, $f_{max}/C=0$;
Case B: $P/D=J$, $f_{max}/C=0.02$, parabolic camber line;
Case C: $P/D=J$, $f_{max}/C=-0.005$, parabolic camber line;
Case D: $P/D=1.1J$, $f_{max}/C=0$.

Figure 6 compares the pitch and camber distributions re-designed by using different initial values as listed above, indicating that the present design method is independent of the blade geometry assumed initially.

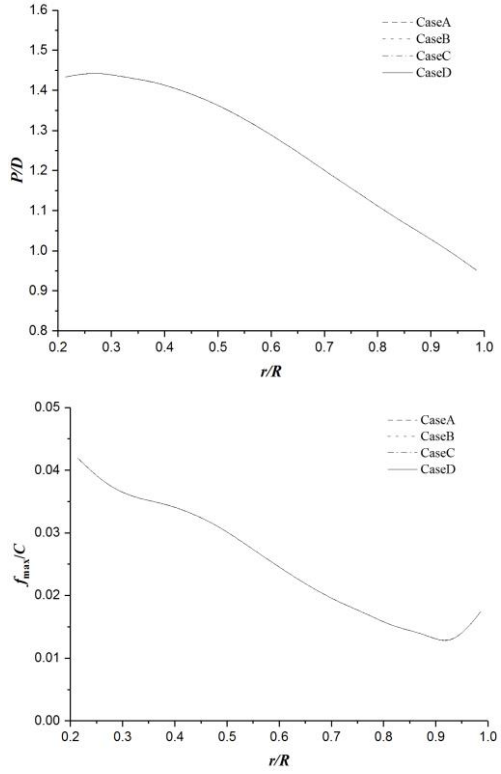

Figure 6. Pitch (upper) and max. camber (lower) distributions re-designed with different initial values.

Figure 7 shows the convergence history of pitch distribution and the camber line shape of a typical section, using the initial values of Case C. The convergence criterion is set as $\varepsilon \leq 10^{-5}$, where ε is the max. error between the non-dimensional circulation $G(r)$ of the designed propeller and the prescribed one, where

$$G(r) = 10^3 \Gamma(r) / \left(\pi D V_{0.7R}\right) \qquad (15)$$

and $V_{0.7R}$ is the undisturbed relative inflow speed at $0.7R$. To satisfy the criterion, more than 200 iterations are needed in this case. The camber line shape converges faster than the pitch distribution.

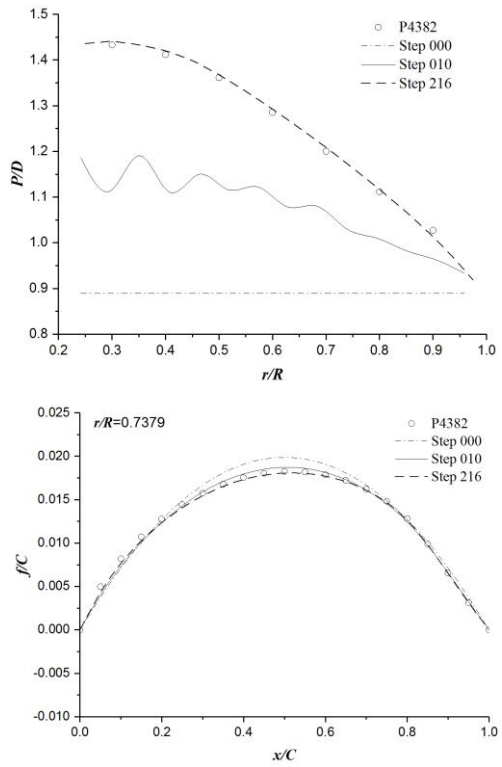

Figure 7. Convergence history of pitch (upper) and camber line shape (lower), using the initial values of Case C.

3.3 Re-design with different circulation distribution

Judging from the circulation distribution predicted by the steady performance solver, it seems that P4382 is a wake-adapted propeller. It would be interesting to see how the geometry differs from that of P4382 if the propeller is designed to have an optimum circulation distribution in the open water. Figure 8 compares the two distributions, where the optimum distribution is given by an in-house lifting-line code, and the corresponding propeller is named as P4382_Opt. Figure 9 compares the pitch and max. camber distributions of P4382 and P4382_Opt. The pitch and camber of P4382_Opt are both lower than those of P4382 when $r/R \leq 0.7$, but higher when $r/R > 0.7$, which is consistent with the differences in circulation distributions.

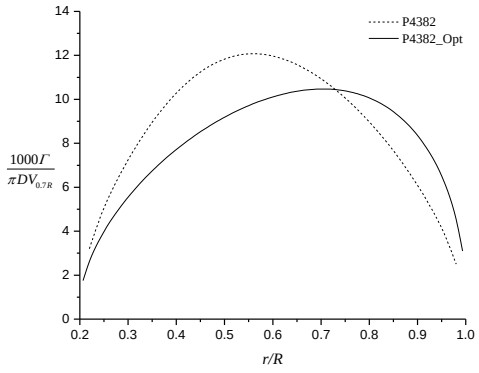

Figure 8. Comparison of circulation distributions.

To verify the design results, numerically at present, the open water performances of P4382_Opt and P4382 are simulated by solving the RANS equations with a well validated numerical setup. The propeller diameter is

0.25m, and the rotational speed is 1200r/min. Figure 10 compares the open water performances, where the open water efficiency of P4382_Opt is slightly (1.9%) higher than that of P4382, as expected. A further comparison is made for the RANS-simulated pressure distributions, as shown in Figure 11, where the differences in pressure jump are also consistent with those in circulation distribution, see Figure 8.

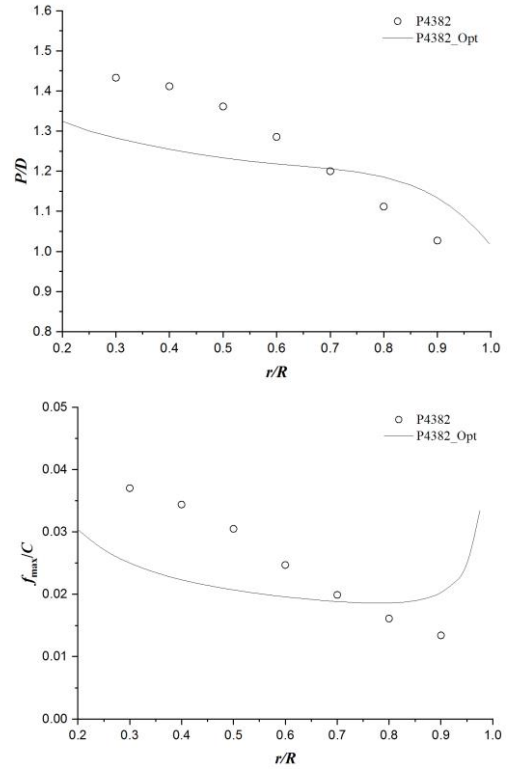

Figure 9. Comparison of pitch (upper) and camber (lower) distributions of P4382_Opt with those of P4382.

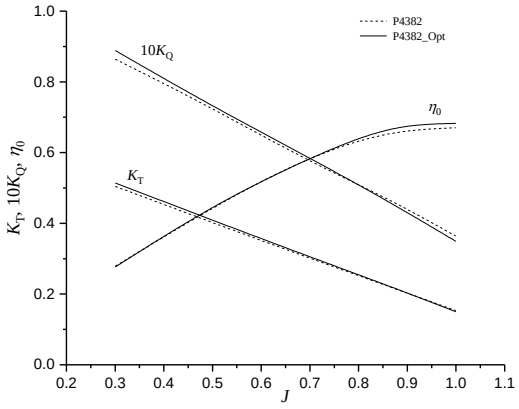

Figure 10. Comparison of open-water performances of P4382_Opt and P4382, both predicted by RANS simulation.

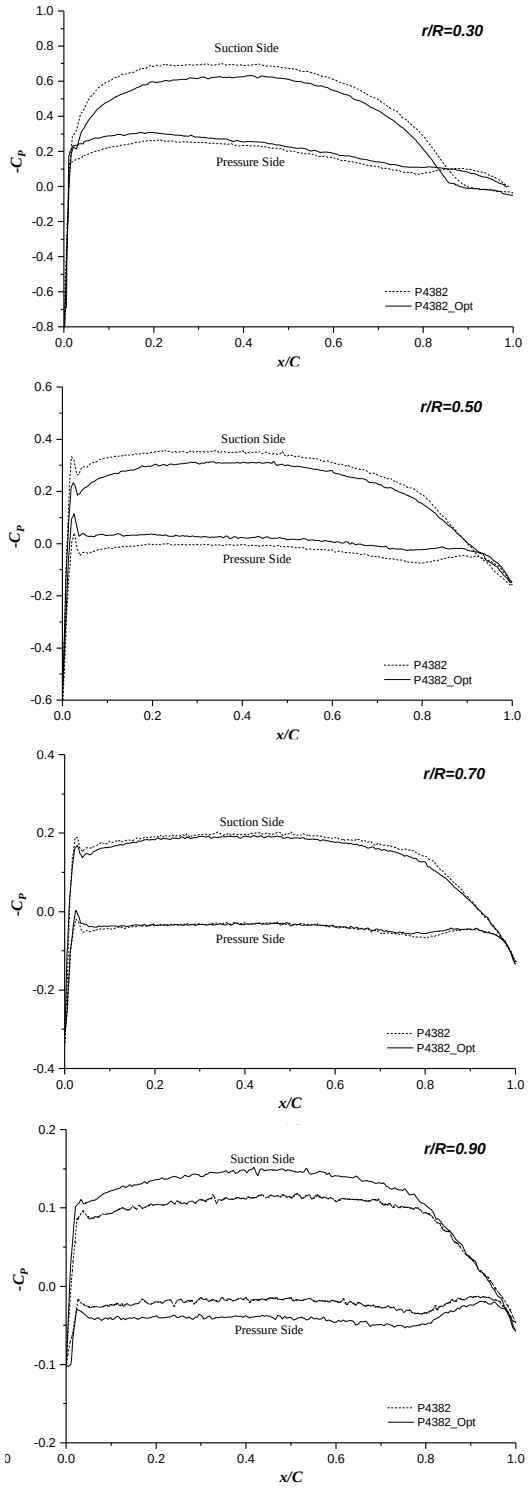

Figure 11. Comparison of pressure distributions of P4382_Opt and P4382, both predicted by RANS simulation.

4 CONCLUSIONS

Based on the vortex lattice lifting-surface model, a new method has been developed to design the ship propeller with a prescribed circulation distribution. The method is based on Newton-Raphson iterations to update the pitch distribution and camber surface geometry, where the circulation distribution is predicted by an in-house VLM solver.

Through numerical examples, it has been shown that the designed pitch and camber distributions converge well with the number of vortex lattices along the span and the chord, and are independent of initial values. The method has also been applied to re-design the prototype propeller with the optimum circulation distribution in open water, and the performance of designed propeller has been verified numerically by RANS simulation.

REFERENCES

Cheng, H. M. (1965). 'Hydrodynamic aspect of propeller design based on lifting-surface theory. Part 2. Arbitrary chordwise load distribution', David Taylor Model Basin, USA.

Greeley, D. S. & Kerwin, J. E. (1982). 'Numerical methods for propeller design and analysis in steady flow', Transactions of the Society of Naval Architects and Marine Engineers, **90**.

Kerwin, J. E. & Lee, C. S. (1978). 'Prediction of steady and unsteady marine propeller performance by numerical lifting-surface theory', Transactions of the Society of Naval Architects and Marine Engineers, **86**.

Kerwin, J. E. & Leopold, R. (1963). 'Propeller incidence correction due to blade thickness', Journal of Ship Research, **7**.

Lerbs, H. W. (1952). 'Moderately loaded propellers with a finite number of blades and arbitrary distribution of circulation', Transactions of the Society of Naval Architects and Marine Engineers, **60**.

Lerbs, H. W. (1955). 'Propeller pitch correction arising from lifting surface effect', David Taylor Model Basin, USA.

Morgan, W. B., Silovic, V. & Denny, S. B. (1968). 'Propeller lifting-surface corrections', Hydro and Aerodynamics Lab., Hydrodynamics Section, Lyngby, Denmark.

Pien, P. C. (1961). 'The calculation of marine propellers based on lifting surface theory', Journal of Ship Research, **5**.

Su, Y. M. & Ikehata, M. (1999). 'A numerical design method of marine propellers using surface panel method', Journal of Kansai Society of Naval Architects, Japan, **231**.

Tan, T.-S. & Xiong, Y. (2005). 'Propeller design by lifting surface theory based on B spline', Journal of Naval University of Engineering, **17**, in Chinese.

Yang, C.-J. & Tamashima, M. (1990). 'A simplified method to predict marine propeller performance including the effect of boss', Transactions of the West-Japan Society of Naval Architects, **80**.